Energy Engineering

Tech Science Press

DOI: 10.32604/ee.2022.019118

ARTICLE

A New Proximity Indicator for Assessment of Voltage Stability and Critical Loadability Point

Chandrakant Dondariya* **and D. K. Sakravdia**

Department of Electrical Engineering, Ujjain Engineering College, Ujjain, India

*Corresponding Author: Chandrakant Dondariya. Email: parth.ckd@uecu.ac.in

Received: 04 September 2021 Accepted: 22 November 2021

ABSTRACT

This paper presents a newly developed proximity indicator for voltage stability assessment which can be used to predict critical real system load and voltages at various load buses at critical loading point. The proximity indicator varies almost parabolic with total real load demand and reaches orthogonally to real load axis. This relation has been utilized to predict critical loading point. It has been shown that two operating points are needed for estimating critical point and proper selection of operating points and variation of proximity indicator near collapse point highly affect the accuracy of estimation. Simulation is based on load flow equations and system real and reactive loadings have been increased in proportion with base case scenario for IEEE 14 and IEEE 25 bus test systems to demonstrate the behaviour of proposed proximity indicator. CPF has been used as benchmark to check the accuracy of estimation.

KEYWORDS

Voltage stability; voltage collapse; proximity indicator; critical loading; CPF

Abbreviations & Symbols

VSM	Voltage stability margin
S_{ϵ}	Substitution error function
PI	Proximity Indicator
P_{LS}	Total real system demand
P_{LC}	Total real demand at critical loading point
V_{iC}	Critical value of i^{th} bus
CPF	Continuation Power Flow

1 Introduction

Transmission of bulk power over long distances using existing network has forced power systems to operate closed to their extreme capabilities. This causes heavy stress even in mature systems and leads to voltage instability. It is always required to have control over voltage in system operation especially when the system is stressed. Voltage stability problem is load driven and considered as a major threat to power system security. Static voltage stability analysis is used to assess the margin to voltage instability

and also to identify weak buses and lines of any system. It helps system planners and operators to identify voltage instability prone areas of the system where attention is needed and also to exercise corrective actions to maintain suitable real and reactive margins in case of heavy loading conditions. Real and reactive power transfer from generators to load buses is the main focus of voltage stability analysis. Continuous monitoring of the system status and fast and accurate determination of proximity to voltage collapse point is a necessary requirement to prevent voltage instability.

In static analysis, power flow simulations have been carried out with various loading conditions. The analysis checks the real and reactive power flows and voltages at various load buses when the system loading has been increased up to critical loading. Static voltage stability may be direct or indirect. P-V and V-Q curves are widely used as a fundamental tool to assess the voltage stability margin (VSM) at any operating point [1]. These curves give direct insight about the voltage stability standing at any load bus. But this needs repetitive simulations and hence significant computational time. Various researchers have proposed indirect static techniques for voltage stability assessment and estimating maximum loadability point. CPF has been a very powerful tool in static voltage stability studies and simulation studies often take reference to results as obtained by CPF [2,3].

Load flow Jacobian which is available at the end of Newton Rapson power flow convergence, contains many useful information about voltage stability and hence it has been area of interest for many researchers. It is well established that Jacobian becomes singular at collapse point [4]. The minimum magnitude of the eigen values of the power flow jacobian matrix is zero at this point [5]. Accurate prediction of collapse point is not possible with these methods because they show very nonlinear behaviour near the critical point [6]. Some researchers have used test functions based on load flow Jacobian for assessment of voltage stability margin by predicting the voltage collapse point using quadratic model [7,8]. Test functions show more reliability than eigen/singular value of Jacobian matrix [9].

In order to have fast and accurate estimation of voltage collapse point, many researchers have proposed various voltage stability indices. A voltage stability index with inverse Jacobian matrix has been proposed in [7], which can be used to estimate voltage stability margin due to its linear behaviour. Maximum elements of system tangent vector has been used in [10] as voltage stability index. When the system is stressed, inverse of the maximum element of tangent vector becomes zero at collapse point. This index can also be used to estimate maximum loadability point [11]. Some researchers have used bus voltages and elements of admittance matrix for checking the system status [12]. Thevenin.s equivalent impedance to load impedances ratio has been taken as proximity indicator by [13], Energy functions have also been considered for estimation of critical power point [14,15]. Tangential angle based voltage stability indicator suitable to complex load models has also been proposed. It can be used for both measurement and model based voltage stability assessment [16]. Artificial neural network based techniques have also been proposed for voltage stability assessment [17]. Bus impedance matrix has also been used for static voltage stability assessment by reducing it to equivalent two bus model [18]. Some authors proposed two bus equivalent system based computation algorithms for assessing active and reactive power limits for voltage stability [19]. PMU measurement based estimation of voltage stability margin has also been proposed [20]. Generalized voltage stability indicator based on tangential angles of PV curves has also been proposed considering voltage dependent load model [21].

2 Problem Identification

Continuous monitoring of the system status and fast and accurate determination of proximity to voltage collapse point is a necessary requirement to prevent voltage instability. Various researchers have

proposed proximity indicators based on load flow Jacobian [4,5,8], Many techniques for the prediction of critical point and maximum loadability margins have also been proposed. It has been established that behavior of proximity indicator near the critical point is the key parameter for accurate estimation of critical point. Linear and parabolic plots of proximity indicator with respect to total real power are in preference for such estimations [8].

The objective of the presented research is to develop a methodology for estimation of critical loading point based on a new proximity index and to investigate accuracy of proposed algorithm.

3 Mathematical Modelling

In static analysis, solution of these of linearised load flow equation is obtained by iterative techniques. It provides a solution in stable operating region. Ill-conditioning of Jacobian based linearised load flowequation results in falling to obtain solution in the stable region. This fact has been utilised for the development of a load flow equations based proximity indicator and the proposed algorithm to investigate voltage stability.

3.1 Derivation of Proposed Proximity Indicator

Consider a set of n linear homogenous equations for

$$[X] = [x_1\, x_2 x_3 \ldots x_n]^T$$

Such that

$$[C][X] = 0 \tag{1}$$

If $[C]$ is non-singular; solution is trivial, i.e., $[X] = 0$

In Eq. (1), Let $x_i = 1$

Excluding i^{th} row equation (i^{th} row of $[C]$) and by solving remaining $(n-1)$ equations for $[X]$, where $n \neq i$, we get a solution

$$[X']_{(n-1)\times 1}$$

Now, i^{th} row equation of Eq. (1) can be written as

$$C_{ii} + \sum_{n\neq i} C_{in} x_n = 0 \tag{2}$$

If $[C]$ is non singular; Eq. (2) will not be satisfied with the solution obtained as Eq. (2) was not considered.

And $x_i = 1$ is an assumed value.

The substitution error function S_ϵ is defined as

$$S_\epsilon = C_{ii} + \sum_{n\neq i} C_{in} x_n \tag{3}$$

It can be seen that if $[C]$ is a singular matrix.

$$S_\epsilon = 0 \tag{4}$$

The concept is applied to load flow Jacobian $[J]$ of the power system network, which becomes singular at voltage collapse point.

Jacobian is computed in N-R load flow solution when the load flow is converged to final solution.

Let $[J]\begin{bmatrix}\Delta\delta\\ \Delta V\end{bmatrix} = \begin{bmatrix}\Delta P\\ \Delta Q\end{bmatrix}$

At solution point, we get linearised power flow equation as

$$[J]\begin{bmatrix}\Delta\delta\\ \Delta V\end{bmatrix} = 0 \tag{5}$$

When the system is stressed up to critical loading, one of the eigen value of load flow jacobian becomes zero and the Jacobian becomes singular.

The substitution error function S_ϵ as given in Eq. (3) will also zero at collapse point.

Hence this function has been taken as proximity indicator for system wise assessment of voltage stability.

$$S_\epsilon = C_{ii} + \sum_{n\neq i} C_{in}x_n \tag{6}$$

As S_ϵ is calculated after the convergence at any loading point, it can be calculated easily from the readily available Jacobian matrix [J] at the end of NR flow solution. This index can be used to assess critical loading of the system.

3.2 Estimation of Critical System Load and Knee Voltage at Load Bus

As discussed earlier, the magnitude of function S_ϵ decrease with increased loading and becomes zero at critical loading. Here, the curve plotted between S_ϵ decreases with increased loading and becomes zero at critical loading. Here the curve plotted between 'S_ε' and 'P_{LS}' is approximated as parabola.

$$P_{LS} = P_{LC} + GS_\epsilon^2 \tag{7}$$

where

P_{LS} = Total system real load

P_{LC} = Load at collapse/critical point

S_ϵ = Substitution error function (proposed proximity indicator)

G = Constant

Let us assume that two system loading conditions are available in stable equilibrium region $[P_{LS1}, V_{i1}, S_{\epsilon 1}]$ and $[P_{LS2}, V_{i2}, S_{\epsilon 2}]$.

V_{i1} and V_{i2} are i^{th} bus voltage at P_{LS1} and P_{LS2} loading conditions, respectively. $S_{\epsilon 1}$ and $S_{\epsilon 2}$ are values of proximity indicates at these loading conditions. The critical load at collapse point can be expressed as

$$P_{LC} = \frac{[P_{LS2}.S_{\epsilon 1}^2 - P_{LS1}S_\epsilon^2]}{[S_{\epsilon 1}^2 - S_{\epsilon 2}^2]} \tag{8}$$

Further, the i^{th} load bus voltage V_i variation is also approximated as parabolic with S_ϵ. Hence V_{iC} at collapse point can be expressed as

$$V_{iC} = \frac{[V_{i2}S_{\epsilon 1}^2 - V_{i1}S_{\epsilon 2}^2]}{[S_{\epsilon 1}^2 - S_{\epsilon 2}^2]} \tag{9}$$

Eqs. (8) and (9) provide the loading condition at critical loading point. It has been shown that the selection of loading condition $[P_{LS1}, V_{i1}, S_{\epsilon 1}]$ and $[P_{LS2}, V_{i2}, S_{\epsilon 2}]$ also affect the accuracy of proposed method. As demonstrated in this paper, two conseutive points very near to collapse have been considered to increase the accuracy of estimation. Fig. 1 shows the flow chart showing proposed algorithm to estimate the critical operating point.

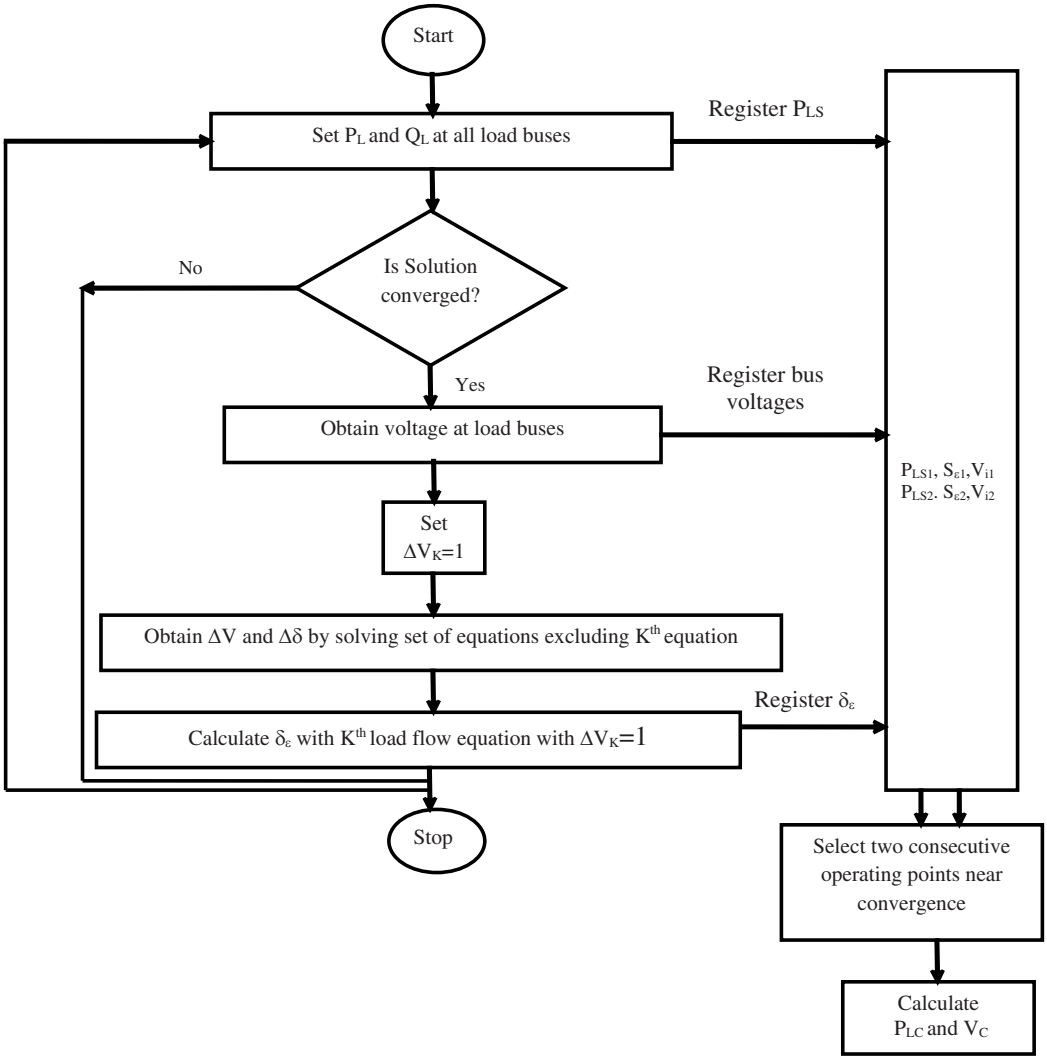

Figure 1: Flow chart for estimating critical loading point

4 Results and Discussion

The developed algorithm has been used to estimate the critical loading point for IEEE 14 bus and IEEE 25 bus test systems [22]. Voltages at each generator bus are set to 1.0 pu. Real and reactive at all load buses have been increased in proportion to base case loading.

The first operating condition is taken as half of base case loading to demonstrate the importance of selection of two loading conditions for enhancing accuracy of estimation of SNBP.

Table 1: Variation in proximity indicator and load bus voltages with total real system loading for IEEE 14 bus test system

Load bus no.	P_{LS}												
	2.045	4.0900	4.4990	4.7035	4.9080	5.1125	5.3170	5.5215	5.7260	5.9305	6.1350	6.3395	6.5440
	PI												
	3.2800	2.7982	2.6719	2.6032	2.5302	2.4518	2.3678	2.2769	2.1779	2.0687	1.9466	1.8077	1.6453
4	0.9491	0.8826	0.8658	0.8568	0.8473	0.8372	0.8266	0.8152	0.8030	0.7898	0.7754	0.7595	0.7414
5	0.9541	0.8941	0.8791	0.8710	0.8626	0.8536	0.8442	0.8342	0.8234	0.8118	0.7992	0.7852	0.7695
6	0.9742	0.9415	0.9334	0.9290	0.9245	0.9197	0.9146	0.9093	0.9036	0.8975	0.8909	0.8837	0.8756
7	0.9541	0.8941	0.8791	0.8710	0.8626	0.8536	0.8442	0.8342	0.8234	0.8118	0.7992	0.7852	0.7695
8	0.9762	0.9453	0.9375	0.9333	0.9289	0.9243	0.9194	0.9142	0.9087	0.9028	0.8963	0.8893	0.8815
9	0.9463	0.8765	0.8592	0.8499	0.8402	0.8299	0.8190	0.8074	0.7951	0.7817	0.7672	0.7511	0.7330
10	0.9427	0.8687	0.8504	0.8405	0.8303	0.8194	0.8079	0.7957	0.7826	0.7686	0.7532	0.7363	0.7172
11	0.9440	0.8715	0.8534	0.8437	0.8336	0.8228	0.8114	0.7993	0.7864	0.7724	0.7571	0.7403	0.7213
12	0.9411	0.8649	0.8459	0.8357	0.8250	0.8136	0.8016	0.7889	0.7752	0.7604	0.7442	0.7264	0.7062
13	0.9388	0.8599	0.8402	0.8296	0.8186	0.8068	0.7944	0.7812	0.7671	0.7519	0.7352	0.7168	0.6959
14	0.9325	0.8457	0.8243	0.8128	0.8008	0.7881	0.7747	0.7604	0.7452	0.7287	0.7107	0.6908	0.6684
Load bus no.	P_{LS}												
	6.6258	6.7076	6.7894	6.8712	6.9530	6.9939	7.0348	7.0757	7.1166	7.1575	7.1984	7.2393	7.2678
	PI												
	1.5714	1.4909	1.4006	1.3000	1.1844	1.1189	1.0467	0.9657	0.8728	0.7627	0.6201	0.4119	0.0011
4	0.7334	0.7249	0.7155	0.7053	0.6940	0.6877	0.6809	0.6735	0.6652	0.6557	0.6439	0.6277	0.5995
5	0.7625	0.7551	0.7470	0.7382	0.7284	0.7230	0.7172	0.7108	0.7037	0.6956	0.6856	0.6719	0.6482
6	0.8721	0.8684	0.8644	0.8600	0.8553	0.8527	0.8499	0.8468	0.8435	0.8397	0.8351	0.8289	0.8185
7	0.7625	0.7551	0.7470	0.7382	0.7284	0.7230	0.7172	0.7108	0.7037	0.6956	0.6856	0.6719	0.6482
8	0.8781	0.8744	0.8705	0.8663	0.8616	0.8591	0.8564	0.8534	0.8501	0.8465	0.8420	0.8360	0.8259
9	0.7250	0.7165	0.7071	0.6970	0.6857	0.6795	0.6728	0.6654	0.6572	0.6479	0.6363	0.6205	0.5929
10	0.7088	0.6998	0.6900	0.6793	0.6674	0.6609	0.6538	0.6461	0.6375	0.6277	0.6155	0.5988	0.5698
11	0.7129	0.7039	0.6941	0.6834	0.6715	0.6649	0.6579	0.6501	0.6415	0.6316	0.6194	0.6026	0.5734
12	0.6972	0.6876	0.6772	0.6658	0.6531	0.6460	0.6385	0.6302	0.6209	0.6103	0.5971	0.5790	0.5472
13	0.6867	0.6769	0.6661	0.6543	0.6412	0.6340	0.6262	0.6176	0.6080	0.5971	0.5834	0.5648	0.5319
14	0.6585	0.6478	0.6362	0.6235	0.6094	0.6016	0.5932	0.5839	0.5736	0.5617	0.5470	0.5267	0.4910

Table 1 shows the variation in proposed proximity indicator and voltage magnitudes of various load buses at various loading conditions for IEEE 14 bus system. As the system is stressed maintaining constant power factor at all load buses, the value of proximity indicator decreases and becomes almost zero near the critical loading condition. It is clear that bus no. 14 has minimum voltage as the proximity indicator approaches to zero. Hence it is the most critical bus from voltage stability viewpoint and needs special attention. Fig. 2 shows the plot of proposed proximity indicator with real system demand 'P_{LS}'. The curve is almost orthogonal near the critical loading. The variation of voltage magnitude of most critical bus is also shown in the same figure for better insight.

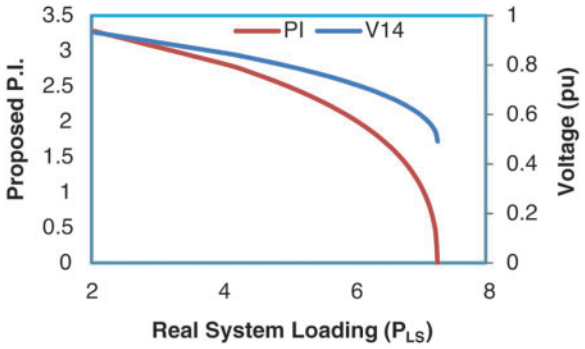

Figure 2: Variation in proximity indicator and voltage V_{14} with total real system load for IEEE 14 bus test system

As discussed, the proposed proximity indicator has been used to estimate the critical loading point of the system. Table 3 shows the values of proximity indicator and voltage magnitude of bus no.14, which is the weakest bus. Two loading conditions are needed to estimate critical loading point for the system. According to [3], which uses CPF method to obtain critical loading condition for IEEE 14 bus test system, suggests that the maximum P_{LS} is 7.3029 and the knee voltage of bus no. 14 is 0.5145. These values have been taken as reference to assess the accuracy of proposed method [3].

As shown in Table 3, two consecutive operating points have been taken to predict maximum loadability point. Percentage errors to estimation are also shown in the Table. It has been found that the accuracy is increased when operating points are taken near to critical loading. Minimum error in estimating maximum real system loading is obtained with loading corresponds to points 20 and 21 and the percentage error is 0.05. Maximum load is estimated as 7.2990 which is very close to that as obtained from CPF. It is also interesting to note that if we take two operating points as 1 and 26, the maximum loadability is calculated as 7.2676 and the percentage error is less than 0.5. These are two loading extremes considered for simulation. Voltage of bus no. 14 has also been estimated based on proposed proximity indicator. Minimum percentage error in estimating voltage at bus no. 14 is 0.74 and the closest value of voltage V_{14} is 0.5107. If half of base case loading point (point 1) and the extreme point near critical point (point 26) have been selected, the percentage error in estimating V_{14} is less than 5%.

Table 2: Variation in proximity indicator and load bus voltages with total real system loading for IEEE 25 bus test system

Load bus no.	P_{LS}														
	3.6500	7.3000	8.7600	10.9500	12.7750	13.5050	14.6000	14.9650	15.3300	15.6950	16.0600	16.4250	16.7900	17.1550	17.5200
	PI														
	4.0485	3.7592	3.6241	3.3931	3.1658	3.0631	2.8921	2.8298	2.7643	2.6954	2.6224	2.5448	2.4621	2.3731	2.2769
6	0.9877	0.9745	0.9690	0.9603	0.9528	0.9498	0.9451	0.9435	0.9419	0.9403	0.9386	0.9370	0.9354	0.9337	0.9320
7	0.9871	0.9716	0.9645	0.9531	0.9425	0.9381	0.9311	0.9287	0.9262	0.9237	0.9211	0.9185	0.9158	0.9131	0.9104
8	0.9861	0.9693	0.9618	0.9496	0.9384	0.9336	0.9262	0.9236	0.9210	0.9183	0.9156	0.9128	0.9100	0.9071	0.9042
9	0.9811	0.9593	0.9497	0.9342	0.9202	0.9143	0.9052	0.9020	0.8988	0.8956	0.8923	0.8889	0.8855	0.8820	0.8785
10	0.9868	0.9711	0.9641	0.9527	0.9424	0.9381	0.9313	0.9290	0.9266	0.9242	0.9217	0.9192	0.9167	0.9141	0.9115
11	0.9858	0.9690	0.9614	0.9492	0.9381	0.9334	0.9261	0.9236	0.9210	0.9184	0.9158	0.9131	0.9104	0.9076	0.9047
12	0.9862	0.9696	0.9621	0.9499	0.9388	0.9340	0.9266	0.9241	0.9215	0.9188	0.9161	0.9134	0.9106	0.9077	0.9048
13	0.9874	0.9740	0.9684	0.9598	0.9523	0.9492	0.9446	0.9430	0.9414	0.9398	0.9382	0.9365	0.9349	0.9333	0.9316
14	0.9697	0.9343	0.9184	0.8923	0.8682	0.8579	0.8414	0.8356	0.8297	0.8237	0.8175	0.8111	0.8045	0.7978	0.7908
15	0.9690	0.9333	0.9175	0.8918	0.8681	0.8580	0.8419	0.8363	0.8306	0.8247	0.8187	0.8125	0.8061	0.7996	0.7928
16	0.9757	0.9479	0.9356	0.9156	0.8973	0.8894	0.8770	0.8727	0.8682	0.8637	0.8590	0.8542	0.8493	0.8442	0.8389
17	0.9874	0.9722	0.9653	0.9540	0.9437	0.9393	0.9324	0.9301	0.9277	0.9252	0.9227	0.9202	0.9176	0.9149	0.9122
18	0.9852	0.9678	0.9600	0.9473	0.9357	0.9308	0.9230	0.9204	0.9176	0.9148	0.9120	0.9091	0.9061	0.9031	0.9000
19	0.9956	0.9897	0.9868	0.9819	0.9773	0.9752	0.9720	0.9708	0.9696	0.9684	0.9672	0.9659	0.9645	0.9631	0.9617
20	0.9849	0.9683	0.9611	0.9497	0.9394	0.9350	0.9281	0.9257	0.9233	0.9208	0.9182	0.9155	0.9128	0.9100	0.9070
21	0.9752	0.9475	0.9354	0.9157	0.8977	0.8899	0.8776	0.8733	0.8688	0.8642	0.8594	0.8545	0.8494	0.8440	0.8385
22	0.9665	0.9285	0.9117	0.8843	0.8588	0.8478	0.8301	0.8238	0.8174	0.8107	0.8037	0.7965	0.7889	0.7810	0.7727
23	0.9794	0.9558	0.9454	0.9282	0.9122	0.9052	0.8940	0.8901	0.8860	0.8818	0.8774	0.8729	0.8682	0.8632	0.8580
24	0.9604	0.9147	0.8942	0.8603	0.8283	0.8142	0.7914	0.7832	0.7748	0.7660	0.7568	0.7471	0.7370	0.7263	0.7150
25	0.9647	0.9233	0.9045	0.8731	0.8431	0.8298	0.8080	0.8002	0.7921	0.7836	0.7748	0.7654	0.7556	0.7452	0.7341

(Continued)

Table 2 (continued)

Load bus no.	P_{LS}													
	17.8850	18.2500	18.6150	18.9800	19.3450	19.7100	20.0750	20.4400	20.5130	20.5276	20.5349	20.5386	20.5393	20.5407	20.5411
	PI														
	2.1719	2.0560	1.9263	1.7772	1.6020	1.3853	1.0911	0.5555	0.3110	0.2077	0.4103	0.0952	0.0846	0.0614	0.0551
6	0.9303	0.9286	0.9269	0.9252	0.9217	0.9199	0.9181	0.9177	0.9176	0.9176	0.9175	0.9175	0.9175	0.9175	0.9175
7	0.9075	0.9046	0.9017	0.8986	0.8923	0.8890	0.8854	0.8846	0.8844	0.8843	0.8843	0.8843	0.8843	0.8842	0.8842
8	0.9012	0.8981	0.8950	0.8917	0.8851	0.8815	0.8778	0.8769	0.8767	0.8766	0.8766	0.8766	0.8765	0.8765	0.8765
9	0.8749	0.8712	0.8675	0.8637	0.8558	0.8517	0.8474	0.8465	0.8463	0.8462	0.8461	0.8461	0.8461	0.8461	0.8461
10	0.9088	0.9060	0.9033	0.9004	0.8946	0.8916	0.8884	0.8878	0.8876	0.8876	0.8875	0.8875	0.8875	0.8875	0.8875
11	0.9019	0.8989	0.8959	0.8928	0.8865	0.8832	0.8797	0.8789	0.8788	0.8787	0.8786	0.8786	0.8786	0.8786	0.8786
12	0.9018	0.8988	0.8957	0.8925	0.8858	0.8823	0.8786	0.8777	0.8775	0.8774	0.8774	0.8774	0.8774	0.8773	0.8773
13	0.9299	0.9282	0.9265	0.9248	0.9213	0.9195	0.9177	0.9173	0.9172	0.9172	0.9172	0.9172	0.9172	0.9172	0.9172
14	0.7836	0.7761	0.7684	0.7604	0.7434	0.7343	0.7249	0.7230	0.7226	0.7225	0.7224	0.7224	0.7224	0.7223	0.7223
15	0.7859	0.7786	0.7712	0.7634	0.7470	0.7382	0.7290	0.7272	0.7268	0.7267	0.7266	0.7266	0.7266	0.7265	0.7265
16	0.8335	0.8279	0.8221	0.8161	0.8033	0.7965	0.7893	0.7879	0.7876	0.7875	0.7874	0.7874	0.7874	0.7874	0.7874
17	0.9095	0.9067	0.9038	0.9009	0.8947	0.8915	0.8880	0.8872	0.8870	0.8869	0.8868	0.8868	0.8868	0.8868	0.8868
18	0.8968	0.8935	0.8902	0.8867	0.8792	0.8751	0.8704	0.8692	0.8688	0.8686	0.8685	0.8685	0.8685	0.8684	0.8684
19	0.9602	0.9586	0.9570	0.9552	0.9514	0.9492	0.9464	0.9455	0.9453	0.9451	0.9450	0.9450	0.9450	0.9449	0.9449
20	0.9040	0.9007	0.8973	0.8937	0.8853	0.8800	0.8725	0.8697	0.8687	0.8681	0.8677	0.8677	0.8676	0.8674	0.8673
21	0.8326	0.8263	0.8196	0.8124	0.7952	0.7841	0.7674	0.7611	0.7587	0.7572	0.7562	0.7562	0.7560	0.7555	0.7554
22	0.7639	0.7545	0.7444	0.7332	0.7066	0.6890	0.6618	0.6514	0.6474	0.6448	0.6431	0.6431	0.6427	0.6419	0.6417
23	0.8526	0.8467	0.8405	0.8338	0.8178	0.8076	0.7926	0.7871	0.7851	0.7838	0.7830	0.7830	0.7828	0.7823	0.7822
24	0.7028	0.6897	0.6755	0.6596	0.6205	0.5937	0.5504	0.5329	0.5260	0.5216	0.5187	0.5187	0.5180	0.5165	0.5161
25	0.7222	0.7093	0.6952	0.6795	0.6403	0.6132	0.5689	0.5508	0.5436	0.5390	0.5360	0.5360	0.5353	0.5338	0.5334

Table 3: Estimation of critical loading (P_{LS}) and voltage at bus no. 14 for IEEE 14 bus test system based on consecutive loading points

Loading point no.	P_{LS}	V14	Sε	P_{LC}	% error P_{LC}	V_{14C}	% error V_{14C}
1	2.0450	0.9325	3.2800	9.5578	−30.8762	0.6136	−19.2655
2	4.0900	0.8457	2.7982				
2	4.0900	0.8457	2.7982	8.7253	−19.4778	0.6032	−17.2334
3	4.4990	0.8243	2.6719				
3	4.4990	0.8243	2.6719	8.5275	−16.7691	0.5978	−16.1821
4	4.7035	0.8128	2.6032				
4	4.7035	0.8128	2.6032	8.4016	−15.0449	0.5958	−15.8009
5	4.9080	0.8008	2.5302				
5	4.9080	0.8008	2.5302	8.2598	−13.1036	0.5926	−15.1879
6	5.1125	0.7881	2.4518				
6	5.1125	0.7881	2.4518	8.1490	−11.5858	0.5891	−14.5056
7	5.3170	0.7747	2.3678				
7	5.3170	0.7747	2.3678	8.0326	−9.9916	0.5848	−13.6655
8	5.5215	0.7604	2.2769				
8	5.5215	0.7604	2.2769	7.9254	−8.5241	0.5817	−13.0657
9	5.7260	0.7452	2.1779				
9	5.7260	0.7452	2.1779	7.8177	−7.0496	0.5764	−12.0369
10	5.9305	0.7287	2.0687				
10	5.9305	0.7287	2.0687	7.7156	−5.6507	0.5716	−11.0941
11	6.1350	0.7107	1.9466				
11	6.1350	0.7107	1.9466	7.6210	−4.3557	0.5661	−10.0287
12	6.3395	0.6908	1.8077				
12	6.3395	0.6908	1.8077	7.5312	−3.1260	0.5603	−8.8956
13	6.5440	0.6684	1.6453				
13	6.5440	0.6684	1.6453	7.4755	−2.3636	0.5557	−8.0004

(Continued)

Table 3 (continued)

Loading point no.	P_{LS}	V14	Sε	P_{LC}	% error P_{LC}	V_{14C}	% error V_{14C}
14	6.6258	0.6585	1.5714				
14	6.6258	0.6585	1.5714	7.4452	−1.9482	0.5513	−7.1565
15	6.7076	0.6478	1.4909				
15	6.7076	0.6478	1.4909	7.4040	−1.3840	0.5490	−6.7149
16	6.7894	0.6362	1.4006				
16	6.7894	0.6362	1.4006	7.3800	−1.0563	0.5445	−5.8307
17	6.8712	0.6235	1.3000				
17	6.8712	0.6235	1.3000	7.3525	−0.6799	0.5405	−5.0591
18	6.9530	0.6094	1.1844				
18	6.9530	0.6094	1.1844	7.3333	−0.4163	0.5369	−4.3485
19	6.9939	0.6016	1.1189				
19	6.9939	0.6016	1.1189	7.3214	−0.2531	0.5343	−3.8565
20	7.0348	0.5932	1.0467				
20	7.0348	0.5932	1.0467	7.3097	−0.0931	0.5307	−3.1473
21	7.0757	0.5839	0.9657				
21	7.0757	0.5839	0.9657	7.2990	0.0531	0.5277	−2.5579
22	7.1166	0.5736	0.8728				
22	7.1166	0.5736	0.8728	7.2896	0.1817	0.5233	−1.7021
23	7.1575	0.5617	0.7627				
23	7.1575	0.5617	0.7627	7.2782	0.3388	0.5183	−0.7453
24	7.1984	0.5470	0.6201				
24	7.1984	0.5470	0.6201	7.2716	0.4287	0.5107	0.7443
25	7.2393	0.5267	0.4119				
25	7.2393	0.5267	0.4119	7.2676	0.4834	0.4918	4.4121
26	7.2676	0.4918	0.0012				

Table 2 shows the variation in proximity indicator and load bus voltages at various loading conditions for IEEE 25 bus system. Real and reactive loads have been increased at all load buses in proportion to base case loading from half of base case load (point 1) till the solution is converged (point 30). Bus no. 24 is identified as weakest bus as it has lowest voltages as the system load is increased.

Fig. 3 shows the graph of proximity index and voltage at weakest bus (bus no. 24) with total real loading (P_{LS}). The curve of proximity indicator approaches to P_{LS} orthogonally as the system real load

obtains its maximum value. CPF suggests the maximum real power demand of the system is 20.4629 pu and the critical voltage at bus no. 24 is 0.5271 pu [3].

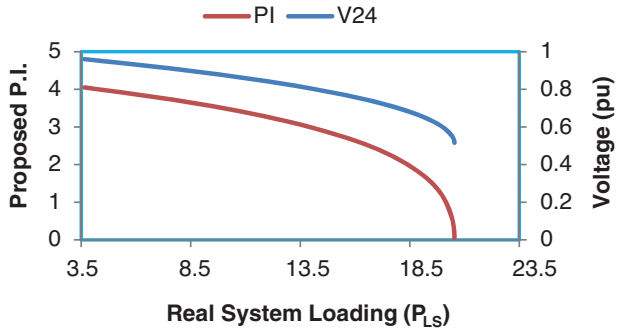

Figure 3: Variation in proximity indicator and voltage V_{24} with total real power load for IEEE 25 bus test system

Estimation of critical loading point has been done with the help of proposed Proximity indicator. As shown in Table 4, two consecutive points have been taken in calculating critical power (P_{LC}) and the voltage of most critical bus (V_{24}). Closest value of critical load is obtained as 20.5394 pu with minimum percentage error of 0.37 between points 23 and 24. The voltage of bus no. 24 calculated between these operating points is 0.5249 and the percentage error is 0.41. If point 1 and point 30 are selected, the estimated critical power is 20.5442 with an error of 0.39%. Voltage at bus no. 24 at critical loading is 0.5160 with an error of 2.1%.

Table 4: Estimation of critical loading (P_{LS}) and voltage at bus no. 24 for IEEE 25 bus test system based on consecutive loading points

Loading point no.	P_{LS}	V_{14}	$S\varepsilon$	P_{LC}	V_{14C}	% error P_{LC}	% error V_{14C}
1	3.6500	0.9604	4.0485	30.1356	0.6288	47.2694	19.2916
2	7.3000	0.9147	3.7592				
2	7.3000	0.9147	3.7592	27.9842	0.6243	36.7556	18.4352
3	8.7600	0.8942	3.6241				
3	8.7600	0.8942	3.6241	26.5047	0.6195	29.5256	17.5340
4	10.9500	0.8603	3.3931				
4	10.9500	0.8603	3.3931	25.0437	0.6132	22.3860	16.3303
5	12.7750	0.8283	3.1658				
5	12.7750	0.8283	3.1658	24.2119	0.6074	18.3209	15.2335

(Continued)

Table 4 (continued)

Loading point no.	P_{LS}	V_{14}	$S\varepsilon$	P_{LC}	V_{14C}	% error P_{LC}	% error V_{14C}
6	13.5050	0.8142	3.0631				
6	13.5050	0.8142	3.0631	23.5939	0.6041	15.3009	14.6139
7	14.6000	0.7914	2.8921				
7	14.6000	0.7914	2.8921	23.1643	0.5990	13.2014	13.6401
8	14.9650	0.7832	2.8298				
8	14.9650	0.7832	2.8298	22.9419	0.5996	12.1145	13.7588
9	15.3300	0.7748	2.7643				
9	15.3300	0.7748	2.7643	22.7444	0.5960	11.1494	13.0795
10	15.6950	0.7660	2.6954				
10	15.6950	0.7660	2.6954	22.5260	0.5938	10.0822	12.6582
11	16.0600	0.7568	2.6224				
11	16.0600	0.7568	2.6224	22.3200	0.5904	9.0754	12.0164
12	16.4250	0.7471	2.5448				
12	16.4250	0.7471	2.5448	22.1335	0.5891	8.1643	11.7696
13	16.7900	0.7370	2.4621				
13	16.7900	0.7370	2.4621	21.9316	0.5863	7.1775	11.2262
14	17.1550	0.7263	2.3731				
14	17.1550	0.7263	2.3731	21.7501	0.5840	6.2905	10.8025
15	17.5200	0.7150	2.2769				
15	17.5200	0.7150	2.2769	21.5709	0.5796	5.4145	9.9603
16	17.8850	0.7028	2.1719				
16	17.8850	0.7028	2.1719	21.3987	0.5767	4.5731	9.4085
17	18.2500	0.6897	2.0560				
17	18.2500	0.6897	2.0560	21.2372	0.5735	3.7839	8.8001
18	18.6150	0.6755	1.9263				
18	18.6150	0.6755	1.9263	21.0677	0.5687	2.9558	7.8837
19	18.9800	0.6596	1.7772				
19	18.9800	0.6596	1.7772	20.9272	0.5641	2.2691	7.0206
20	19.3450	0.6417	1.6020				

(Continued)

Table 4 (continued)

Loading point no.	P_{LS}	V_{14}	$S\varepsilon$	P_{LC}	V_{14C}	% error P_{LC}	% error V_{14C}
20	19.3450	0.6417	1.6020	20.7920	0.5577	1.6085	5.7964
21	19.7100	0.6205	1.3853				
21	19.7100	0.6205	1.3853	20.6714	0.5499	1.0191	4.3270
22	20.0750	0.5937	1.0911				
22	20.0750	0.5937	1.0911	20.5677	0.5352	0.5122	1.5461
23	20.4400	0.5504	0.5555				
23	20.4400	0.5504	0.5555	20.5463	0.5249	0.4077	−0.4154
24	20.5130	0.5329	0.3110				
24	20.5130	0.5329	0.3110	20.5394	0.5204	0.3736	−1.2626
25	20.5276	0.5260	0.2077				
25	20.5276	0.5260	0.2077	20.5410	0.5179	0.3818	−1.7440
26	20.5349	0.5216	0.1403				
26	20.5349	0.5216	0.1403	20.5418	0.5162	0.3854	−2.0631
27	20.5386	0.5187	0.0952				
27	20.5386	0.5187	0.0952	20.5419	0.5154	0.3862	−2.2251
28	20.5393	0.5180	0.0846				
28	20.5393	0.5180	0.0846	20.5423	0.5148	0.3878	−2.3277
29	20.5407	0.5165	0.0614				
29	20.5407	0.5165	0.0614	20.5428	0.5144	0.3902	−2.4008
30	20.5411	0.5161	0.0551				

In view of above results, it can be concluded that proposed proximity indicator is useful in estimating the maximum loadability of the system and voltages at various load buses at critical point. The approximation of S_{ε}-P_{LS} plots as parabolic works well if two operating points taken are very near to collapse point and preferably near to convergence limit of NR power flow program. The estimation is even fair if half of base case loading point (light loading) and operating point of last convergence are taken.

5 Conclusion

This paper has proposed a new load flow equation based proximity indicator and simulation study has been carried out with the help of developed algorithm (Fig. 1) by considering IEEE 14 bus and IEEE 25 bus test systems to demonstrate the behaviour of proposed proximity indicator as the system load is increased till the convergence of NR based load flow program, The P_{LS}-S_{ε}

plots obtained for both systems are approximated as parabolic as seen in Figs. 2 and 3 and hence an approximate relationship has been formulated between system active load and proximity indicator. Voltage magnitudes at all load buses are also recorded and bus 14 is identified as weakest bus in IEEE 14 bus system (Table 1) and bus 24 is identified as weakest bus in IEEE 25 bus test system (Table 2).

For estimation of critical power and voltage two loading points are taken and computed values of proximity index at these points are used. It has been concluded from Tables 3 and 4 that for both the test systems, the accuracy of estimating critical power and critical voltage at the weakest bus is increased when the points are taken near the point of last convergence of NR based load flow program,

With the work in this paper, it is concluded that:

- The proximity index variation with system loading can be approximated as regular curve.
- Linear and parabolic plots are suitable for simple and quick estimation of critical loading point.
- The variation of proximity indicator near critical point and its close matching with the approximated curve is the key factor for accurate prediction of critical loading point on PV curve.
- Accuracy of estimation could be increased by taking two loading points near the point of extreme convergence of NR load flow program.

As the voltage stability phenomenon is load driven and depends upon how system reactive power varies with real system power, the proportionate load increase scenario as taken only give only an insight. Load P-Q characteristics can vary at each load bus and must be considered in simulation for accurate prediction with the proposed algorithm.

6 Future Scope

To avoid voltage instability, continuous system monitoring and accurate prediction of critical loading point is necessary. In this study, two operating points preferably near the point of last convergence are taken to reduce the error in estimating critical point with the help of proposed proximity indicator. Newton's divided difference formula can also be used by selected more number of points. Artificial neural networks can also be used to predict the collapse point. Load P-Q characteristics must be considered in simulation to improve the accuracy of estimation.

Acknowledgement: We are very thankful to Administration of Ujjain Engineering College Ujjain, India, Faculty and Staff of Department of Electrical Engineering, Ujjain Engineering College, Ujjain, India and RGPV Bhopal India providing us all support to complete this research work. Valuable guidance from Dr. L. D. Arya, Retd. Professor, S.G.I.T.S Indore, India is also acknowledged.

Funding Statement: The author declare that no specific funding has been received for this study.

Conflicts of Interest: The authors declare that they have no conflicts of interest to report regarding the present study.

References

1. Taylor, C. W. (1994). *Power system voltage stability.* New York: McGraw Hills.
2. Eady, S. I., Christy, C. (1992). The continuation power flow: A tool for steady state voltage stability analysis. *Institute of Electrical and Electronics Engineers. Transactions on Power Systems, 7,* 416–423. DOI 10.1109/59.141737.

3. Arya, L. D., Sakravdia, D. K., Choubey, S. C. (2003). Continuation power flow with tangent predictor and pseudo-arc length parameterization. *Journal of the Institution of Engineers (India): Electrical Engineering Division, 83,* 291–295.
4. Gao, B., Morison, G. K., Kundur, P. (1992). Voltage stability evaluation using modal analysis. *Institute of Electrical and Electronics Engineers Transactions on Power Systems, 7(4),* 1529–1541. DOI 10.1109/59.207377.
5. Lof, P. A., Smed, T., Andersson, G., Hill, D. J. (1992). Fast calculation of a voltage stability index. *Institute of Electrical and Electronics Engineers Transactions on Power Systems, 7(1),* 54–64. DOI 10.1109/59.141687.
6. Berizzi, A., Finazzi, P., Dosi, D., Marannino, P., Corsi, S. (1998). First and second order methods for voltage collapse assessment and security enhancement. *Institute of Electrical and Electronics Engineers Transactions on Power Systems, 13(2),* 543–551. DOI 10.1109/59.667380.
7. Chiang, H. D., Jumeau, R. J. (1995). Toward a practical performance index for predicting voltage collapse in electric power systems. *Institute of Electrical and Electronics Engineers Transactions on Power Systems, 10(2),* 584–592. DOI 10.1109/59.387892.
8. Arya, L. D., Sakravdia, D. K., Choube, S. C. (2001). Development of a proximity indicator and its application for estimating maximum loadability point. *Journal of Institution of Engineers (India), 82,* 87–91.
9. Canizares, C. A., De Souza, A. C. Z., Quintana, V. H. (1996). Comparison of performance indices for detection of proximity to voltage collapse. *Institute of Electrical and Electronics Engineers Transactions on Power Systems, 11(3),* 1441–1450. DOI 10.1109/59.535685.
10. Chen, K., Hussein, A., Bradley, M. E., Wan, H. (2003). A Performance-index guided continuation method for fast computation for saddle-node bifurcation in power systems. *Institute of Electrical and Electronics Engineers Transactions on Power Systems, 18(2),* 753–760. DOI 10.1109/TPWRS.2003.811203.
11. Kessel, P., Glavitsch, H. (1986). Estimating the voltage stability of a power system. *Institute of Electrical and Electronics Engineers Transactions on Power Systems, 1(3),* 346–354. DOI 10.1109/TPWRD.1986.4308013.
12. Balamourougan, V., Sidhu, T. S., Sachdev, M. S. (2004). Technique for on line prediction of voltage collapse. *IEE Proceedings-Generation, Transmission and Distribution, 151(4),* 453–460. DOI 10.1049/ip-gtd:20040612.
13. Chebbo, A. M., Irving, M. R., Sterling, M. J. H. (1992). Voltage collapse proximity indicator: Behaviour and implications. *IEE Proceedings (Generation, Transmission and Distribution), 139,* 241–252. DOI 10.1049/ip-c.1992.0037.
14. Cifci, A., Uyaroglu, Y., Yalcin, M. A. (2012). Voltage stability via energy function analysis on reduced order model of power system. *Turkish Journal of Electrical Engineering & Computer Science, 20(1),* 1031–1043. DOI 10.3906/elk-1105-12.
15. Overbye, T. J., Demarco, C. L. (1991). Improved techniques for power system voltage stability assessment using energy methods. *Institute of Electrical and Electronics Engineers Transactions on Power Systems, 6,* 1446–1452. DOI 10.1109/59.116988.
16. Hecke, V. J., Hatziargyriou, N. D., van, C. T. (1994). *Indices predicting voltage collapse including dynamic phenomena*, vol. 91, pp. 91–94. CIGRE: Paris, France, http://www.montefiore.ulg.ac.be/services/stochastic/pubs/1994/HHV94.
17. Salama, M. M., Saied, E. M., Abou-Elsaad, M. M., Ghariany, E. F. (2001). Estimating the voltage collapse proximity indicator using artificial neural network. *Energy Conversion and Management, 42(1),* 69–79. DOI 10.1016/S0196-8904(00)00023-6.
18. Lee, D. H. A. (2016). Voltage stability assessment using equivalent nodal analysis. *Institute of Electrical and Electronics Engineers Transactions on Power Systems, 31(1),* 454–463. DOI 10.1109/TPWRS.2015.2402436.
19. Haque, M. H. (1995). A fast method for determining the voltage stability limit of a power system. *Electric Power Systems Research: Hecke, 32(1),* 35–43. DOI 10.1016/0378-7796(94)00893-9.

20. Su, H., Liu, C. (2016). Estimating the voltage stability margin using PMU measurements. *IEEE Transactions on Power Systems, 31(4),* 3221–3229. DOI 10.1109/TPWRS.2015.2477426.
21. Kamel, M., Li, F., Bu, S., Wu, Q. (2021). A generalized voltage stability indicator based on the tangential angles of PV and load curves considering voltage dependent load models. *International Journal of Electrical Power & Energy Systems, 127,* 106624. DOI 10.1016/j.ijepes.2020.106624.
22. Wallach, Y. (1986). *Calculations and programs for power system networks*. PHI.